IL NUOVO CIMENTO Vol. 36 C, N. 4 Luglio-Agosto 2013
DOI 10.1393/ncc/i2013-11542-2

Communications: SIF Congress 2012

Growth and characterization of epitaxial ultrathin-Fe on $BaTiO_3$ films

C. Rinaldi(*)

LNESS-Dipartimento di Fisica, Politecnico di Milano - Via Anzani 42, 22100 Como, Italy

ricevuto il 31 Dicembre 2012

Summary. — Interfacial multiferroics have recently emerged as a promising way to circumvent the lingering scarcity of room-temperature multiferroics. First-principles calculations have predicted such interfacial multiferroics to exhibit magnetoelectric coupling and interface-induced multiferroicity, both at room temperature, if robust ferroics such as Fe and $BaTiO_3$ are combined together. In order to understand the physics of magnetoelectric coupling effects at the Fe/$BaTiO_3$ interface, a precise knowledge of the atomic-scale structural, magnetic and chemical properties is fundamental. In this paper, the growth of fully epitaxial ultrathin Fe layers on $BaTiO_3$ films is presented. By means of *I-V* measurements we demonstrate the ferroelectricity of 150 nm thick $BaTiO_3$ films grown by pulsed-laser deposition on $La_{2/3}Sr_{1/3}MnO_3$//$SrTiO_3$(001). Furthermore, X-ray absorption spectroscopy and X-ray magnetic circular dichroism measurements have been acquired on epitaxial Co/Fe(2-3 MLs)/$BaTiO_3$ structures at the Fe $L_{2,3}$ edges, giving a direct evidence for the presence of a non-magnetic iron oxide monolayer between $BaTiO_3$ and the remaining layers of the ultrathin Fe, which are magnetic.

PACS 77.55.fe – $BaTiO_3$-based films.
PACS 77.55.Nv – Multiferroic/magnetoelectric films.
PACS 75.50.Bb – Fe and its alloys.
PACS 75.70.Ak – Magnetic properties of monolayers and thin films.

1. – Introduction

The design of room-temperature multiferroic materials and nanoscale architectures currently generates strong theoretical and experimental efforts in condensed-matter physics as well as in the development of upcoming spintronic devices [1]. For instance, multiferroics showing strong magnetoelectric coupling could lead to spin-based devices

(*) On behalf of G. Radaelli; E-mail: christian.rinaldi@mail.polimi.it

with ultralow power consumption and novel microwave components. In the case of independent switching of the ferroic order parameters, multiferroics could also find applications as multiple-state data storage elements. However a room-temperature multiferroic material is still missing. In this contest is particularly promising the integration in nanoelectronic devices of interfacial multiferroics with magnetoelectric coupling and interface-induced multiferroicity, both at room temperature, achieved by the combination of robust ferroics such as Fe and $BaTiO_3$ (BTO). Examples of such nanoelectronic devices include artificial tunnel junctions (MFTJs) in which magnetic and spin-dependent transport properties can be electrically controlled in a non-volatile way, enabling low-power information write operations in magnetic random access memories [2]. These heterostructures combine ferromagnetic (FM) electrodes and a ferroelectric (FE) insulator as the tunnel barrier. The resistance of such devices is expected to depend on the magnetic and ferroelectric orders, *i.e.*, they display Tunnel MagnetoResistance (TMR) and Tunnel ElectroResistance (TER) effects, respectively, giving rise to four different resistance states. As previously said, the pivotal point in such nanojunctions is the presence of magnetoelectric phenomena at FE/FM interface.

These interfacial magnetoelectric effects may come out as a modulation of the magnetic moments of Fe and the spin polarization induced by the ferroelectricity at the FE/FM interface and by the corollary induction of a finite magnetic moment in the FE. Interface mechanisms at the origin of such magnetoelectric coupling have been theoretically predicted to be mediated by hybridization of spin-polarized electronic states at the common interface [3] or by spin-dependent screening of the ferroelectric polarization of BTO in the interfacial FM layer [4]. Recently, Garcia *et al.* [5] demonstrated the nonvolatile electrical control of the TMR in artificial $La_{2/3}Sr_{1/3}MnO_3/BaTiO_3/Fe$ (LSMO/BTO/Fe) MFTJs by switching the electrical polarization of the tunnelling barrier: a modulation of the carriers spin polarization is obtained by changing the direction of FE polarization. More recently, experimental evidence of remanent induced magnetic moments on Ti and O atoms coupled with those of Fe was observed in analogous LSMO/BTO/Fe MFTJs by means of X-ray resonant magnetic scattering (XRMS) measurements [6]. However, these averaging real-space techniques are not sensitive enough to probe pure atomic and electronic interfacial properties in those artificial MFTJs, where the Fe film thickness is 5 nm. Both X-ray absorption spectra and the related magnetic dichroism were typical of bulk bcc Fe. Moreover, the quality of Fe films is relatively poor, since it consists of textured crystallites. Despite this, atomically resolved STEM-HAADF images of these samples have proved useful to suggest a description of the Fe/BTO interface structure different from that previously theoretically indicated [3], *i.e.*, where an additional iron oxide monolayer seems to be intercalated between BTO and Fe [6, 7]. However, in view of the extreme sensitivity of both tunneling and induced magnetic moments to the interface details, a precise knowledge of the atomic scale structures, but also of the magnetic configuration of Fe at the interface, is a prerequisite to understand the physics of multiferroics junctions and, more in general, of magnetoelectric coupling effects at FM/FE interfaces.

In this contest, the preparation and characterization of high-quality ultrathin Fe films on ferroelectric BTO films is a fundamental achievement. Pioneering experimental work has been done by Brivio *et al.* [8]: high-quality 1–3 nm thick Fe films have been epitaxially grown on BTO/STO(001). However, the preparation of ultrathin Fe films (thickness of few monolayers) on BTO films bears a challenge from the experimental side. In fact, there are still questions to be addressed concerning the chemical structure and the magnetic order of the Fe/BTO interface. As suggested before [6, 7], oxidation of Fe

at the interface is expected due to the chemical bonding with BTO. Moreover, since Fe has the tendency toward antiferromagnetism if the volume is reduced, we expect a complex magnetic structure at the Fe/BTO interface in dependence of the structure Fe-film thickness, which depends strongly on the interface structure [9]. Recently, first-principles calculations have been employed to predict X-ray Absorption Spectra (XAS) and X-ray Magnetic Circular Dichroism (XMCD) of 1 to 3 MLs thick Fe layers on a TiO_2-terminated BTO(001) surface [10]. These calculations show a different magnetic behaviour of Fe as a function of its thickness, suggesting the need to employ XAS and XMCD to understand the complex magnetic properties of Fe at the interface with BTO.

In this paper we demonstrate the epitaxial growth of ultrathin Fe (2–3 MLs thick) films on ferroelectric BTO (150 nm thick) films for the study of interfacial properties. By means of *I-V* measurements, we demonstrate the epitaxial growth of ferroelectric 150 nm thick BTO films on LSMO//STO(001). Moreover, we take advantage of the element selectivity of X-ray absorption spectroscopy and XMCD to provide direct evidence of a single non-magnetic iron oxide layer lying between BTO and ferromagnetic ultrathin Fe.

2. – Experimental details

The samples growth and *in situ* characterization have been performed in an ultrahigh vacuum (UHV) system equipped with a molecular-beam-epitaxy (MBE) apparatus, a chamber for pulsed-laser deposition (PLD) and one for electron spectroscopies, as described in details elsewhere [11]. For this study, BTO/LSMO(50 nm)//STO(001) and Fe/BTO/LSMO(50 nm)//STO(001) heterostructures have been grown. PLD was used to deposit both LSMO and BTO, while MBE was used for the Fe deposition. In every sample the thickness of the BTO layer was 150 nm. For XAS and XMCD experiments, the ultrathin Fe layer (2–3 MLs thick) was capped by Au(4 nm)/Co(1 nm) and the BTO was unpoled.

The first investigated sample is based on BTO/LSMO bilayer grown by PLD on (001)-oriented STO substrate in the dedicated chamber. The growth of conductive LSMO layer is necessary to have a bottom electrode to polarize BTO, since STO substrates are insulating. The growth parameters for BTO have been optimized following indications of previous work [12], in order to obtain high-quality epitaxial ferroelectric films with low surface roughness, which is a fundamental requirement in order to obtain high-quality Fe/BTO interface. Before of the growth, an annealing of the substrate up to 730 °C is performed for cleaning and ordering the surface, the temperature being controlled by a pyrometer. A quadrupled Q-Switched Nd:YAG laser (266 nm), providing pulses 7 ns long with a fluence of 5.2 J/cm^2 (for LSMO deposition process) and 2.2 J/cm^2 (for BTO deposition process), has been operated at a repetition frequency of 2 Hz to generate a plasma from a stoichiometric target placed in front of the substrate at a distance of 40 mm (for LSMO deposition process) or 30 mm (for BTO deposition process). 50 nm LSMO films have been grown at a deposition temperature of 730 °C and an oxygen pressure of 0.22 Torr. The subsequent growth of BTO with an oxygen pressure of 0.02 Torr has been performed at 640 °C. The deposition rate in these conditions is 0.15 Å/pulse for LSMO and 0.18 Å/pulse for BTO, as deduced from RHEED oscillations and confirmed by thickness measurements on different BTO and LSMO films by X-Ray Reflectometry (XRR) using a PANalytical PRO-MRD high-resolution triple-crystal diffractometer (data not shown). After deposition of the bilayer, a post-annealing of 30 min at 600 °C in a high oxygen pressure (760 Torr) has been performed in order to avoid oxygen vacancies in the BTO and to improve the surface structural quality, the latter checked afterward by the

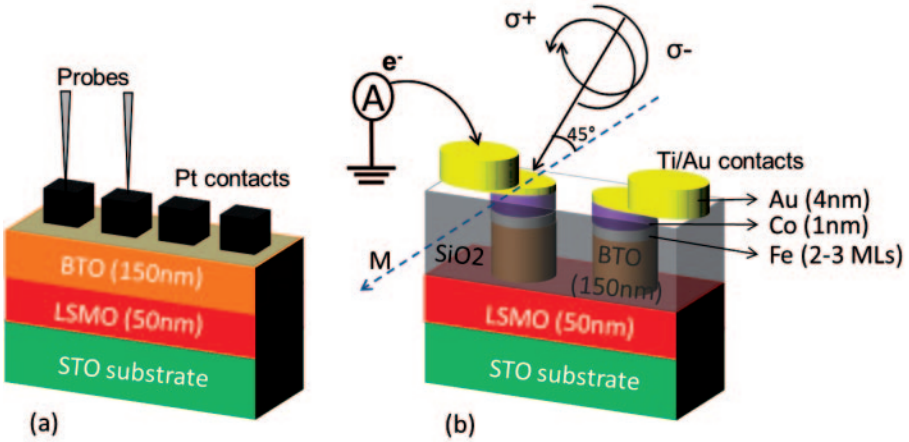

Fig. 1. – (a) Sketch of the samples structure for the ferroelectric characterization of BTO. (b) Structure of the sample and geometry for XMCD measurements on an ultrathin Fe layer (2–3 monolayers). Circularly polarized X-rays impinges on the Au/Co/Fe/BTO pillars at 45° with respect to the sample surface. The current generated by the absorption of X-rays and photoemission of core electrons has been measured with a picoammetter connected to the sample.

appearance of Low Energy Electron Diffraction (LEED) pattern. Ferroelectricity of BTO film has been investigated by means of *I-V* measurements at 10 kHz, and P-E loops have been obtained by the integration of the current through time. Leakage contribution has been removed by using the dielectric leakage current compensation (DLCC) [13]. These measurements have been performed in top-top configuration, which means between two different Pt contacts (thickness 60 μm; area 0.035 mm^2) deposited on the BTO surface *ex-situ* by sputtering (fig. 1a).

For the study of magnetic and chemical properties of Fe at the interface with BTO, ultrathin Fe films (2–3 MLs thick) have been grown *in situ* by MBE on previously described BTO(150 nm)/LSMO(50 nm)//STO(001) heterostructures. For XAS and XMCD experiments the sample has been capped *in situ* with Au(4 nm)/Co(1 nm) deposited by MBE. All the process has been performed in UHV conditions with the substrate kept at RT. The pressure during the deposition process was always in the 10^{-10} Torr range. A movable shutter available in the deposition chamber has been used for covering half of the surface of the sample during the deposition of the last monolayer of Fe, in order to obtain on the same sample two zones with different Fe thickness, 2 and 3 MLs, respectively. After the deposition of Fe layer a 20 min post-annealing at 200 °C has been performed in order to improve the structural quality of Fe. The deposition rates for Fe, Co and Au have been calibrated with a quartz microbalance and then checked by *in situ* X-ray photoemission spectroscopy (XPS). *Ex situ* XAS and XMCD experiments have been performed at room temperature at APE beamline of the ELETTRA synchrotron radiation source in Trieste (Italy) for chemical analysis and magnetic characterization of the interface. XAS and XMCD are state-of-the-art methods to determine both the electronic and magnetic structures of materials. In addition to the element selectivity of XAS, XMCD gives information on the spin and orbital magnetic moment of the excited atoms. XMCD originates from coupling between the photon spin and the atomic magnetic moments, which gives rise to a difference between the absorption cross sections

measured with the magnetic field parallel or antiparallel to the photon wave vector. For these measurements, the sample has been patterned with optical lithography and ion beam etching processes in order to define separated structures of 1 mm^2 area for each Fe thickness. Additional optical lithographic and lift-off processes have been performed to fill with insulating capping SiO_2 layer the space between defined structures and finally to evaporate Au(200 nm)/Ti(15 nm) contacts to electrically connect the structures leaving part of the surface free for X-ray absorption measurements (fig. 1b). XAS spectra of the $L_{2,3}$ edge of Fe and Co have been collected in total electron yield (TEY) with fast scan mode (changing the incoming photon energy in a continuous way and at the same time measuring the sample drain current by means of a picoammitter connected to the surface of the sample, for a fixed light polarization and magnetization direction). The angle of incidence of the incoming light has been fixed at 45° with respect to the sample surface, as shown in fig. 1b. The magnetic field is applied along one of the two-fold Fe easy axis. To avoid the influence of the magnetic field on the TEY acquisition, data have been obtained in magnetic remanence.

For each magnetization direction, the spectrum has been obtained as an average of a high number of scans, in order to obtain four high-quality spectra, combination of the light circular polarization ($\sigma+$ or $\sigma-$) and magnetization direction ($\mu-$ for negative and $\mu+$ for positive magnetization with respect to the easy axis). Afterwards, the spectra I corresponding to $(\mu-, \sigma+)$ and $(\mu+, \sigma-)$, and $(\mu-, \sigma-)$ and $(\mu+, \sigma+)$ have been summed to obtain the two dichroic spectra I with parallel (P) and antiparallel (AP) alignment between photon polarization and magnetization (this step helps eliminating instrumental asymmetry due to residual stray field):

$$I_P = I(\mu-, \sigma+) + I(\mu+, \sigma-), \tag{1}$$

$$I_{AP} = I(\mu-, \sigma-) + I(\mu+, \sigma+). \tag{2}$$

The dichroic quantity is defined as $A_{XMCD} = (I_P - I_{AP})/(I_P + I_{AP})$. In the case of non-magnetic atoms, I_P and I_{AP} are expected to be equal and, thus, $A_{XMCD} = 0$.

3. – Results and discussion

The first step of this work has been the PLD growth of BTO/LSMO films on STO(001) substrates. The lattice mismatch between LSMO and STO (0.83%) generates an in-plane tensile strain on the LSMO film in case of cube-on-cube epitaxial growth. This structural deformation relaxes as soon as the thickness of the film increases. The lattice mismatch between BTO and LSMO, determined by the strain level of LSMO, is quite high (−2.18% in case of LSMO fully strained by the STO substrate; −2.98% in case of LSMO fully relaxed) and consequently BTO films grow on LSMO under in-plane compressive strain in case of cube-on-cube epitaxial growth, with an elongation of the tetragonal in the out-of-plane direction, leading to a sizable enhancement of the dielectric polarization of BTO [14]. In fig. 2, the results of FE characterization performed in top-top configuration (fig. 1a) on 150 nm thick BTO film grown on LSMO(50 nm)//STO(001) are shown. Ferroelectric loops P-E (panel a) and I-E (panel b) at 10 kHz show that the BTO film is ferroelectric, with quite high saturation polarization (P_S about 35 μC/cm^2) and remanent polarization (P_R about 28 μC/cm^2) values. Note that this polarization value is larger than in the bulk BTO (26 μC/cm^2), suggesting that the BTO film, even being very thick, is still under compressive strain due to the LSMO//STO substrate.

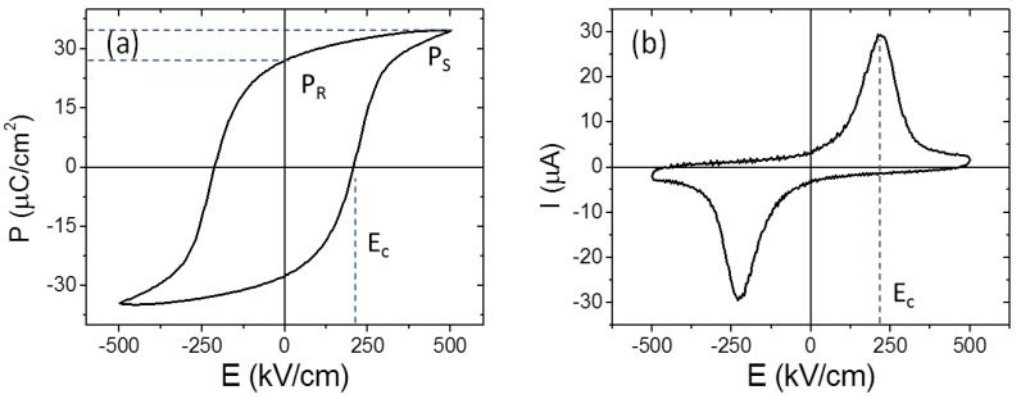

Fig. 2. – Ferroelectric loop P-E (a) and I-E (b) for the BTO(150 nm)/LSMO(50 nm)//STO(001) sample measured at a frequency of 10 kHz. The DLCC compensation technique has been used to subtract the leakage current contribution. BTO shows quite high saturation polarization (P_S is about 35 μC/cm^2) and remanence polarization (P_R is about 28 μC/cm^2). The ferroelectric coercive field E_C is about 240 kV/cm.

A preliminary X-Ray Diffraction (XRD) analysis showing the presence of both the strained and relaxed component of BTO (data not showed) confirms the presence of strain within the BTO layer. Moreover, measurements of retained polarization after delay time show that almost all the polarization (negatively and positively pre-poled) is retained and stable in time, at least for the maximum delay of 100 s achieved during these measurements (data not shown). The ferroelectric properties of the BTO film represent the starting point for the occurrence of magnetoelectric coupling but they are still not enough: the crystalline quality and the reduced roughness of the surface of the BTO film are other fundamental requirements in order to obtain nearly ideal FE/FM interfaces. With our growth recipe, the BTO/LSMO bilayer appears to grow epitaxially with cube-on-cube mode on STO(001) substrates. Figure 3 shows a LEED pattern taken with electron energy of 75 eV on a 150 nm BTO film. The (100) and (010) spots lie along the (100) and (010) axis of the STO substrate, so that the epitaxial relationship between BTO and STO is BTO[100]//STO[100], as expected from the minimization of the elastic energy due to the lattice mismatch. Furthermore, relatively low roughness of BTO surface is confirmed by AFM analysis which gives a RMS value of 0.17 nm on a $1 \times 1\,\mu$m^2 area (data not shown).

The high quality of the BTO surface is a good starting point for the growth and the study of an epitaxial Fe/BTO interface. Fe films with a thickness within the range 2–3 MLs have been grown by MBE on BTO/LSMO//STO(001) heterostructures, according to the receipt described above. In this case, the sample has been capped with Au(4 nm)/Co(1 nm) layers. The Au layer has been used in order to prevent the oxidation of the metallic layers underneath once the sample is exposed to air. On the contrary, the 1 nm thick Co layer (with bulk-like magnetic signal shown in fig. 4) is expected to help in stabilizing epitaxy and magnetization of the ultrathin Fe film, which otherwise could prefer a paramagnetic nanoparticles configuration. According to the lattice mismatch, Fe films are expected to grow with cubic structure presenting a 45° rotation of

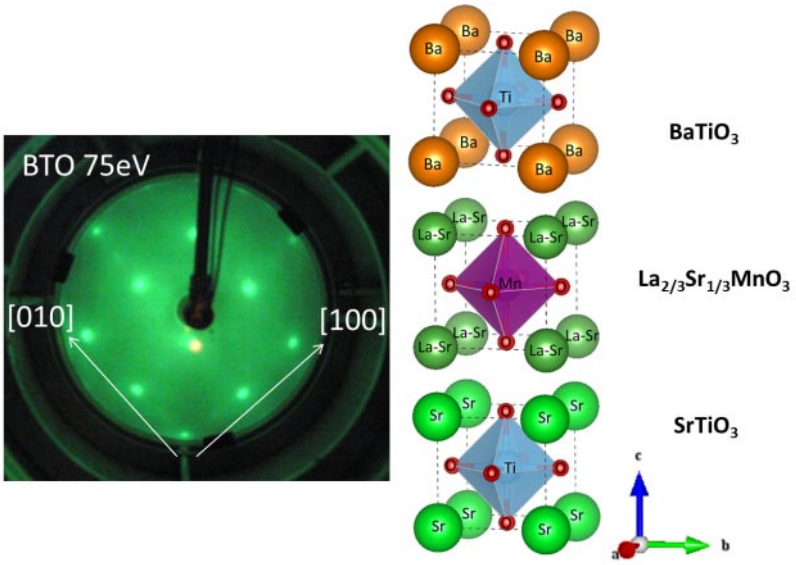

Fig. 3. – LEED pattern taken with electron energy of 75 eV on a 150 nm thick BTO film grown on LSMO(50 nm)//STO(001). The (100) and (010) spots correspond to the two sides of the STO substrate, so that the epitaxial relationship between BTO and STO is BTO[100]//STO[100], as expected according to the lattice mismatch. On the right, the resulting crystal structure for the full BTO/LSMO/STO stack is shown. The a, b and c axes correspond to the directions STO(100), STO(010) and STO(001), respectively.

the lattice respect to the BTO one, so that the epitaxial relationship between Fe and BTO is Fe[100]//BTO[110] [8]. The oxidation of Fe during the interface formation can be investigated looking at the lineshape of Fe L_2 and L_3 peaks. Figures 4c and 4d show the I_P and I_{AP} absorption spectra, after background subtraction of, respectively, 3 and 2 MLs thick Fe films grown on BTO. Metallic Fe gives the characteristic broad and asymmetric doublet peaks coming from absorption from $2p_{1/2}$ and $2p_{3/2}$ levels to $3d$ level at 719.9 and 706.8 eV, respectively. However, the measured spectra presents also doublet peaks shifted at higher photon energies which give rise to the formation of a shoulder on the main peaks. These peaks, located around 723 and 710 eV, can be attributed to the oxidation of iron. This shoulder is more evident in the thinner Fe film (2 MLs). This finding indicates the presence of oxidized iron at the interface, most probably, over solely one atomic layer, the one which is chemically bonded to the BTO.

This finding confirms also for high-quality epitaxial growth a more complex atomic and electronic structure of the studied interface than the ideal model considered in earlier theoretical studies [3, 9, 10], consisting of a TiO_2-terminated surface with interfacial apical O atoms aligned along the Fe sites. In the panel e of fig. 4, the dichroic signal A_{XMCD} of 2 and 3 MLs thick Fe film is shown. In both cases a non-zero signal appears in correspondence of metallic Fe peaks, with intensity ratio between L_3 and L_2 peaks which is consistent with bulk Fe one, while no dichroic signal has been measured in correspondence to the oxide iron peaks. These findings reveal the non-magnetic nature of the oxide iron layer present at the interface between Fe and BTO. Despite this, the successive Fe layers show a metallic bulk-like magnetic signal.

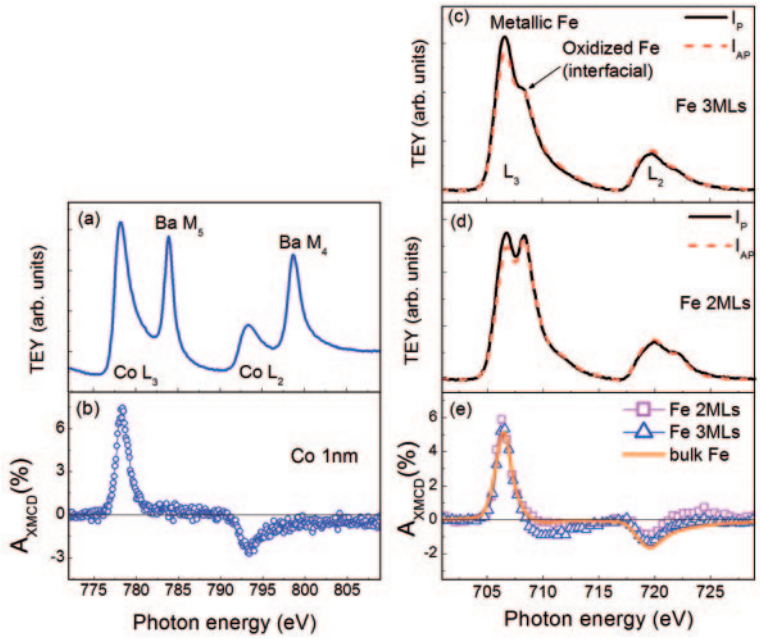

Fig. 4. – (Color online) (a) X-ray absorption spectra ($I_P + I_{AP}$) for the Co $L_{2,3}$ edges. (b) Dichroic signal (A_{XMCD}) of the Co 1 nm thick film. Note that in the same energy range, also the $M_{4,5}$ edges of Ba are present (panel a), but they do not give a magnetic contribution to A_{XMCD} (panel b). On the right, X-ray absorption spectra (after background subtraction) for parallel (I_P) and antiparallel (I_{AP}) alignment between the photon polarization and the magnetization for an Fe film of 2 MLs (panel c) and 3 MLs (panel d). The corresponding dichroic signal (A_{XMCD}) is compared with a reference bulk Fe (orange line) in the panel (e).

4. – Conclusions

In summary, the growth of fully epitaxial ultrathin Fe films on ferroelectric BTO films has been demonstrated. *I-V* measurements show that our 150 nm thick BTO films grown on LSMO(50 nm)//STO(001) are ferroelectric, with quite high saturation polarization (35 μC/cm^2) and remanent polarization (28 μC/cm^2) values, and retention time. Moreover, LEED and AFM analysis confirm crystalline quality and reduced roughness of the surface of the BTO film, which represent fundamental requirements to obtain ideal FE/FM interfaces. Finally, XAS and XMCD analysis of epitaxial ultrathin Fe (2–3 MLs thick) films, sandwiched between 1 nm thick magnetic Co layer and 150 nm thick ferroelectric BTO layer, have been performed to understand the magnetic and chemical properties of the interface BTO/Fe. Our analysis show the presence of a non-magnetic iron oxide monolayer at the very interface between Fe and BTO, covered by the subsequent bulk-like magnetic Fe layers. While theoretical predictions of magnetoelectric coupling mechanism take into account a very simple ideal interface between Fe and BTO, these findings will hopefully stimulate new theoretical works and considerations on the magnetoelectric coupling at FE/FM interfaces, taking into account the more complex atomic, chemical and magnetic structure of the actual Fe/BTO interface found in this paper.

* * *

This work was supported by Fondazione Cariplo via the project EcoMag (Project No. 2010-0584). The paper has been written in behalf of G. Radaelli of the same institution. The author acknowledge R. Bertacco, D. Petti, M. Leone of LNESS centre, Dipartimento di Fisica of Politecnico di Milano for working in this project. D. Chrastina of the LNESS centre, Dipartimento di Fisica of Politecnico di Milano for XRR and XRD measurements. P. Torelli and G. Panaccione from APE beamline at ELETTRA synchrotron (Trieste) for assistance during XAS and XMCD experiments. I. Fina, D. Gutierrez and J. Fontcuberta from Institut de Ciència de Materials de Barcelona (ICMAB-CSIC, Campus UAB, Bellaterra, Spain) for BTO ferroelectric characterization.

REFERENCES

[1] Bibes M., *Nat. Mater.*, **11** (2012) 354.
[2] Bibes M., Villegas J. E. and Barthlmy A., *Adv. Phys.*, **60** (2011) 5.
[3] Duan C-G., Jaswal S. S. and Tsymbal E. Y., *Phys. Rev. Lett.*, **97** (2006) 047201.
[4] Cai T., Ju S., Lee J., Sai N., Demkov A. A., Niu Q., Li Z. and Shi J., *Phys. Rev. B*, **80** (2009) 140415.
[5] Garcia V., Bibes M., Bocher L., Valencia S., Kronast F., Crassous A., Moya X., Enouz-Vedrenne S., Gloter A., Imhoff D., Deranlot C., Mathur N. D., Fusil S., Bouzehouane K. and Barthlmy A., *Science*, **327** (2010) 1106.
[6] Valencia S., Crassous A., Bocher L., Garcia V., Moya X., Cherifi R. O., Deranlot C., Bouzehouane K., Fusil S., Zobelli A., Gloter A., Mathur N. D., Gaupp A., Abrudan R., Radu F., Barthlmy A. and Bibes M., *Nat. Mater.*, **10** (2011) 753.
[7] Bocher L., Gloter A., Crassous A., Garcia V., March K., Zobelli A., Valencia S., Enouz-Vedrenne S., Moya X., Mathur N. D., Deranlot C., Fusil S., Bouzehouane K., Bibes M., Barthlmy A., Colliex C. and Stphan O., *Nano Lett.*, **12** (2012) 376.
[8] Brivio S., Rinaldi C., Petti D., Bertacco R. and Sanchez F., *Thin Solid Films*, **519** (2011) 5804.
[9] Fechner M., Maznichenko I. V., Ostanin S., Ernst A., Henk J., Bruno P. and Mertig I., *Phys. Rev. B*, **78** (2008) 212406.
[10] Borek St., Maznichenko I., Fischer G., Hergert W., Mertig I., Ernst A., Ostanin S. and Chass A., *Phys. Rev. B*, **85** (2012) 134432.
[11] Bertacco R., Cantoni M., Riva M., Tagliaferri A. and Ciccacci F., *Appl. Surf. Sci.*, **252** (2005) 1754.
[12] Radaelli G., Brivio S., fina I. and Bertacco R., *Appl. Phys. Lett.*, **100** (2012) 102904.
[13] Fina I., Fbrega L., Langenberg E., Mart X., Snchez F., Varela M. and Fontcuberta J., *J. Appl. Phys.*, **109** (2011) 074105.
[14] Choi K. J., Biegalski M., Li Y. L., Sharan A., Schubert J., Uecker R., Reiche P., Chen Y. B., Pan X. Q., Gopalan V., Chen L. Q. and Schlom D. G., *Science*, **305** (2004) 1005.